



# Assessing leachate contamination and groundwater vulnerability in urban dumpsites: a case study of the Ipata Area, Ilorin, Nigeria

N. K. Olasunkanmi<sup>a,\*</sup>, D. T. Ogundele<sup>b</sup>, V. T. Olayemi<sup>b</sup>, W. A. Yahya<sup>a</sup>, A. R. Olasunkanmi<sup>c</sup>, Z. O. Yusuf<sup>a</sup>, S. A. Aderoju<sup>d</sup>

<sup>a</sup>Physics and Materials Science Department, Kwara State University, Malete, Nigeria

<sup>b</sup>Chemistry and Industrial Chemistry Department, Kwara State University, Malete, Nigeria

<sup>c</sup>Department of Environmental Impact Assessment and Management, School of Environmental, Education and Development, University of Manchester, United Kingdom

<sup>d</sup>Department of Statistics and Mathematics, Kwara State University, Nigeria

## Abstract

This study explores the extent of leachate contamination and groundwater vulnerability in urban dumpsites, with a specific focus on the Ipata area in Ilorin, Nigeria. The study employs a combination of 2D Electrical Resistivity Tomography (ERT), soil classification, and physicochemical analyses to investigate the percolation of leachate into groundwater and its potential environmental and health implications. The ERT data unveiled subsurface layers, highlighting the presence of decomposed topsoil down to approximately 1.2m. Beneath this layer, a low-resistivity zone (6.53 to 10.7  $\Omega$ m) indicated the potential risk of leachate percolation into groundwater. Soil classification revealed a shallow topsoil layer with insufficient clay content to hinder leachate penetration, emphasizing the need for enhanced containment measures. Physicochemical analysis of leachate, well water, and soil displayed variations in key parameters such as pH, electrical conductivity, total dissolved solids, and anion concentrations. Leachate exhibited high pH and electrical conductivity, suggesting elevated total dissolved solids, while well water remained within acceptable pH limits for drinking water. Heavy metal concentrations exceeded permissible WHO limits in topsoil, leachate, and well water, with cadmium presenting a high ecological risk. The absence of persistent organic pollutants (POPs) in the samples indicates a current focus on heavy metals as a primary concern. In conclusion, this study underscores the urgent need for proactive pollution abatement measures in urban dumpsites like Ipata. Regular monitoring of surface and groundwater quality is essential to safeguard public health and the environment.

DOI:10.46481/jnsps.2024.1889

**Keywords:** Leachate contamination, Soil classification, Sustainable waste management, Groundwater quality monitoring

## Article History :

Received: 04 November 2023

Received in revised form: 29 November 2023

Accepted for publication: 25 March 2024

Published: 21 April 2024

© 2024 The Author(s). Published by the Nigerian Society of Physical Sciences under the terms of the Creative Commons Attribution 4.0 International license. Further distribution of this work must maintain attribution to the author(s) and the published article's title, journal citation, and DOI.

Communicated by: M. M. Orosun

## 1. Introduction

Leachate, particularly from dumpsites, poses a significant threat to shallow aquifer contamination [1]. The migration of leachate raises concerns for human health and the environment due to its potential to contaminate aquifers and surface wa-

\*Corresponding author: Tel. No.: +234-803-437-0033.  
Email address: [nurudeen.olasunkanmi@kwasu.edu.ng](mailto:nurudeen.olasunkanmi@kwasu.edu.ng) (N. K. Olasunkanmi)

ters over extended periods [2–5]. This is especially worrisome when industrial waste is involved, as leachate often contains harmful substances including fulvic acids, organic carbon, and hazardous chemicals. Originally located outside metropolitan areas, dumpsites have expanded due to urbanization and population growth, encroaching upon nearby land that now hosts public or residential structures. Unconfined landfills pose a significant threat to both surface water and groundwater resources [2, 6–8]. In less developed countries like Nigeria, shallow aquifers are crucial drinking water sources, exposing humans to the percolation of contaminated leachate.

The decomposition byproducts of solid waste may permeate the ground and seep into groundwater, especially in areas with specific topography, hydrology, and rock types [1, 9]. Leachates can travel both vertically and horizontally, potentially contaminating groundwater, surface water, soil, and rocks [10]. Monitoring wells are an effective but expensive way to study leach plume movement [11]. Considering that leachate plumes often follow specific paths determined by subsurface heterogeneity, geophysical techniques offer a more efficient approach. Geophysical methods, like 2D Electrical Resistivity Tomography (ERT), are employed to investigate contaminant plumes, locate preferential flow paths, and monitor injected chemicals for remediation [12, 13]. ERT, a well-established approach, aids in assessing contaminants, landfill studies, and groundwater contaminant investigations [14–16]. It has been used to detect pollution, identify geo-electric layers, confirm geotechnical stability, and more [17–23].

While soil contamination often focuses on chemical aspects, integrating geophysical, geochemical, and sometimes microbial analyses is essential [24–27]. Dumped waste at the Ipata dumpsite mainly originates from commercial and residential activities Figure 1, containing pollutants like nutrients, heavy metals, and organic materials. The inorganic components may dissolve in groundwater due to interactions with geological materials. Factors like local temperature and moisture content influence leachate composition and volume. pH plays a crucial role in water quality and chemical reactions, affecting metal toxicity and solubility [28]. Polycyclic Aromatic Hydrocarbons (PAHs) are significant organic contaminants, posing threats due to their persistence and harmful characteristics. PAHs help decipher hydrogeochemical processes underlying groundwater chemistry changes.

The hydrological conditions near the Ipata dumpsite are susceptible to contamination. Factors such as water movement through rocks, recycling through irrigation, and natural/artificial recharge and discharge influence groundwater chemistry. Water composition changes due to interactions with lithological and stratigraphic features, leading to distinct hydrochemical facies. To protect those living near the dumpsite, regular assessments of leachate migration to groundwater in the Ipata area are crucial. This study aims to identify leachate contamination, assess its depth in the auriferous zone, determine soil's contribution to leachate movement, and evaluate soil contamination through physicochemical parameters and ecological risk assessment.



Figure 1. Aerial View of Ipata area showing the Open Dumpsite, a sample pit position, and some sample hand-dug wells.

### 1.1. Geological setting and Location of the Study Area

Geologically, the Ilorin area rests upon South-Western Nigeria's Precambrian Basement Complex, primarily composed of metamorphic and igneous rock types Figure 2. The waste dumpsite predominantly lies atop a migmatite-gneiss complex within the southwestern basement, characterized by varying thicknesses of weathered regolith [29]. This area is within the Precambrian Basement Complex of Nigeria known as Dahomeyan Shield that was part of rejuvenated rocks between the West African and Congo Cratons which belongs to the pre-drift Pan African mobile belt [30]. The hydrological context mirrors other Basement Complex regions, where water availability is linked to clay-rich overburden and water-filled joints, fractures, or faults in the underlying basement rocks, possibly acting as groundwater conduits. The study site, Ipata, spans latitudes 8° 29' 40" N to 8° 30' 50" N and longitudes 4° 33' 00" E to 4° 34' 50" E. Hosting the bustling Ipata market, it accommodates around 1,622,438 inhabitants across an estimated 295-square-mile area. The climate in Ilorin is Tropical Savanna, characterized by distinct wet and dry seasons and mild weather. Artificial drainage effectively manages water runoff in the area. The temperature ranges from 33–34 °C (November to January) and 34–53 °C (February to April). Mean monthly temperatures average between 25–28.9 °C. Ilorin experiences variable rainfall patterns, both in terms of time and location [29].

## 2. Methodology

### 2.1. Electrical Resistivity Survey and Soil Classification

The Electrical Resistivity method, utilizing the Wenner Electrode configuration, was employed to investigate subsurface resistivity distribution with the aim of mapping lithologic units around the Ipata dumpsite and identifying geologic structures conducive to leachate migration. The survey encompassed four profiles within the dumpsite: three parallel profiles oriented in the W-E direction and one perpendicular profile in the

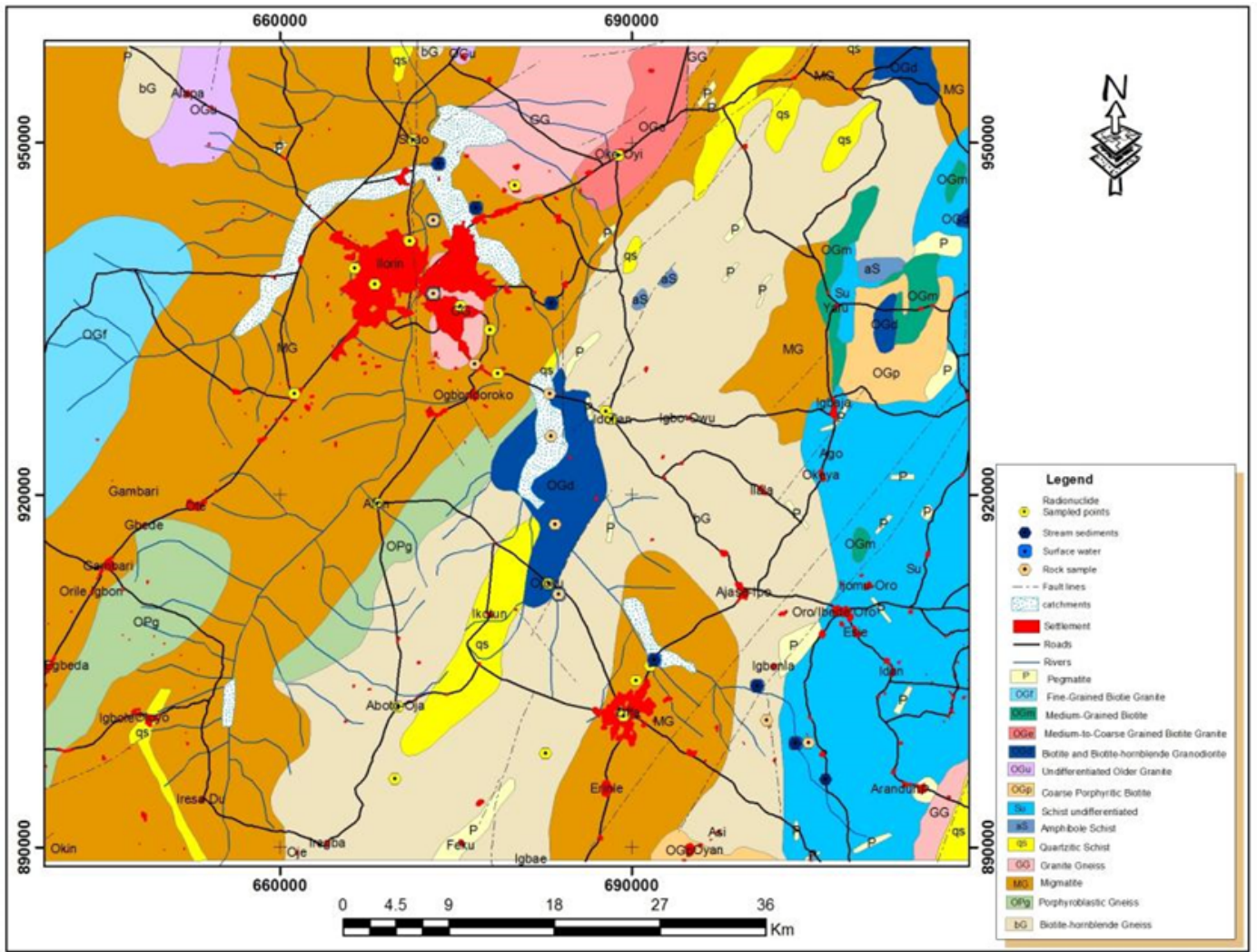


Figure 2. Geological map of Ilorin showing the study area.

N-S direction. The profiles spanned approximately 120–150 m, adjusted according to the area’s topography and accessibility. Utilizing a 2D resistivity imaging technique, the survey aimed to illustrate lateral resistivity distribution within the dumpsite. Electrode spacing ranged from 1.0 m to 10.0 m, with ABEM SAS3000 digital electrical resistivity meter capturing the data. The measured resistance was converted to apparent resistivity using equation 1, involving the Wenner geometric factor ( $G_w$ ).

$$\rho_a = 2\pi a \cdot \frac{\Delta V}{I} = G_w \cdot R, \quad (1)$$

where ‘a’ is the electrode spacing at each point and ‘ $\rho_a$ ’ is apparent resistivity, and

$$G_w = 2\pi a. \quad (2)$$

Subsequently, the apparent resistivity data sets underwent a transformation into 2D inverse resistivity models through the RES2DINV inversion code [31]. This code employs a smoothness-restricted least squares approach to automatically

generate 2D resistivity models from the input data. In electrical resistivity tomography (ERT), crucial information regarding unknown parameters such as resistivity values and layer depth is pivotal for inversion processing [31].

In conjunction with the resistivity survey, vertical pits were manually excavated at anomalous points along the traverses. These sampling locations were strategically positioned to encompass the dumpsite’s perimeter and other significant areas Figure 3 a-d. Around 12 disturbed soil samples were collected from the test-dug pits, with depths limited to 0 - 3.0 m. The collected soil samples were placed in individual polythene sacs, meticulously labeled for proper identification, and rid of impurities following standard procedures. These soil samples were then preserved and transported to the University of Ilorin Geology Departmental Laboratory for thorough testing and characterization. Evaluations included natural moisture content, Atterberg limit, linear shrinkage, and grain size analysis following the British standard institute BSI 1377 (1990) soil classification standard.



Figure 3. Vertical pitting showing near-surface lithologic sequence beneath Ipata Market dumpsite around the dumpsite, non-degradable waste materials (topsoil), and near-surface leachate.

## 2.2. Physicochemical properties test

The physico-chemical properties of the (surface and subsurface soil, leachate, and shallow well water) samples were assessed using standard methods as outlined in APHA, 2005. For elemental composition analysis via Atomic Absorption Spectroscopy, samples underwent preparation according to Anton Pear's multi-wave 3000 microwave digestion system adaptation. Dissolution involved adding precisely 0.2 g of soil or 10 mL of water sample into digestion flasks, followed by the addition of concentrated nitric acid  $\text{HNO}_3$ . Heating was employed until near dryness, with further additions of hydrochloric acid  $\text{HCl}$  and perchloric acid  $\text{HClO}_4$ , followed by another round of heating and the addition of concentrated  $\text{HCl}$ . The digested samples were filtered and transferred into pre-cleaned 100 mL polypropylene vials, diluted with distilled water for AAS analysis. The analysis covered elements such as As, Cr, Co, Fe, Mn, Ni, Pb, Cd, Cu, and Zn. All chemical reagents utilized were of laboratory grade.

Regarding polluted soil and water samples, they were prepared for gas chromatography-mass spectrometry (GC/MS) following the modified USEPA method 827 °C. Weighing 5 g of the sample 5 mL of extract, and 5 g of anhydrous sodium sulfate, the mixtures were homogenized. The mixture was transferred to pre-cleaned extraction tubes, where 40 mL of dichloromethane was added. After standing for 30 minutes, the tubes were shaken vigorously for another 30 minutes. Solids settled, and solvent layers were filtered using paper filters. A repetition of the procedure with 25 mL of dichloromethane fol-

lowed, with the combined extracts concentrated using a rotary evaporator (Buchi Rotavapor R-114). After an exchange with 10 mL of n-hexane, the extracts were concentrated to 1 mL for cleanup. Cleaned extracts were subjected to elution using 40 mL dichloromethane/hexane on a silica gel column. These extracts were evaporated, redissolved in 1 mL n-hexane, and analyzed for the 16 representative PAHs utilizing a Shimadzu GC/MS QP 2010 model.

## 2.3. Soil Contamination

Metal concentrations of the selected study areas were assessed to determine the levels of contamination of the study locations. Table 1 shows the heavy metals concentration in topsoil, Leachate and well water to determine the level of penetration of the contaminants. Contamination Factor (CF) indicates contamination resulting from human activities of a single heavy metal [32]. It is a ratio between the concentration of each heavy metal in the soil and geochemical background value of such metal. CF is calculated by equation (3).

$$CF = \frac{\text{Concentration of the metal in soil}}{\text{Background value}} \quad (3)$$

The heavy metal geochemical background value (mg/kg) used for this study are As = 13, Cr = 90, Fe = 47,200, Pb = 85, Co = 20, Cd = 0.8, Zn = 140, Ni = 35, Cu = 36 and Mn = 850 [33–35]. Contamination values are classified into four:  $CF < 1$  (low contamination),  $1 < CF < 3$  (moderate contamination),  $3 < CF < 6$  (considerable contamination) and  $CF > 6$  (very high contamination) [33]. Pollution Load Index (PLI) is used to evaluate the overall heavy metal pollution status of a particular site and it is determined using equation (4) [36].

$$PLI = [CF_1 \times CF_2 \times CF_3 \dots \times CF_N]^{\frac{1}{N}}, \quad (4)$$

where 'N' is the number of metals studied and CF is the contamination factor. A  $PLI < 1$  indicates uncontaminated;  $PLI = 1$  presents that only baseline levels of pollutants are present, and  $PLI > 1$  is polluted [36]. Geo-accumulation Index ( $I_{geo}$ ) estimates heavy metal load resulting from anthropogenic or geogenic inputs to the soil. It is determined using equation (5) [37]

$$I_{geo} = \log_2 \left[ \frac{C}{1.5B} \right], \quad (5)$$

where: 'C' is heavy metal content in soil and 'B' is background value of each metal. The  $I_{geo}$  was classified into seven classes: unpolluted ( $I_{geo} \leq 0$ ), unpolluted to moderately polluted ( $0 < I_{geo} \leq 1$ ), moderately polluted ( $1 < I_{geo} \leq 2$ ), moderately to heavily polluted ( $2 < I_{geo} \leq 3$ ), heavily polluted ( $3 < I_{geo} \leq 4$ ), heavily to extremely polluted ( $4 < I_{geo} \leq 5$ ) and extremely polluted ( $I_{geo} > 5$ ) [35, 38, 39] Ecological Risk Factor (E) quantitatively expresses the potential ecological risk of a given single contaminant [31] and is given as equation (6).

$$E = T \times CF, \quad (6)$$

where T is toxic response factor of a particular heavy metal (Arsenic = 10, Cadmium = 30, Chromium = 2, Cobalt = 2,

Table 1. Heavy metal concentrations in topsoil, underground soil, and well water of Ipata Market.

Sample Location	Heavy Metals	concentration (mg/kg)SD	WHO limits
Sample A Top Soil	As	51.7±0.05	0.5
	Cd	12.3±0.004	0.8
	Cr	21.7±0.003	100
	Co	11.7±0.01	0.01
	Cu	4.5±0.001	36
	Fe	142.3±0.004	445
	Mn	21.6±0.005	0.5
	Ni	7.95±0.004	35
	Pb	21.6±0.002	85
Zn	39.4±0.03	50	
Sample B Leachate	As	18.5±0.007	0.5
	Cd	13.95±0.002	0.8
	Cr	76.5±0.004	100
	Co	13.6±0.001	0.01
	Cu	42.7±0.004	36
	Fe	681.7±0.004	445
	Mn	52.2±0.002	0.5
	Ni	11.6±0.003	35
	Pb	43.7±0.004	85
Zn	72.3±0.001	50	
Sample C Well Water	As	11.1±0.004	0.5
	Cd	0.1±0.004	0.8
	Cr	1.43±0.014	100
	Co	0.1±0.003	0.01
	Cu	1.0±0.005	36
	Fe	142.6±0.014	445
	Mn	1.5±0.003	0.5
	Ni	0.1±0.002	35
	Pb	1.6±0.014	85
Zn	1.6±0.004	50	

Copper = 5, Iron = 1, Manganese = 1, Nickel = 5, Lead = 5 and Zinc = 1) [34, 35, 39, 40] and CF is the contamination factor. The ecological risk factors are classified as follows:  $E < 40$  - low potential ecological risk;  $40 \leq E < 80$  - moderate potential ecological risk;  $80 \leq E < 160$  - considerable potential ecological risk;  $160 \leq E < 320$  - high potential ecological risk and  $E \geq 320$  - very high ecological risk [31]. Potential Ecological Risk Index (RI) estimates the overall harmful effects of different heavy metals in soil [31] using Equation 7. RI are classified as: Low risk ( $RI < 150$ ), moderate risk ( $150 \leq RI < 300$ ), high risk ( $300 \leq RI < 600$ ) and very high risk ( $RI \geq 600$ ) [31, 41]

$$RI = \sum E. \quad (7)$$

### 3. Result and discussion

The results from the tomographic sections (Figures 4a – 4d) exhibit three distinct images for each profile. These images include (a) the plot of measured (observed) apparent resistivity

pseudo-section, (b) the calculated apparent resistivity pseudo-section, and (c) the resistivity model obtained after a specific number of inversion program iterations. Additionally, the figures showcase the positions of shallow hand-dug wells, septic tanks, and their corresponding locations on the profiles. The sections highlighted distinctive zones of relatively low and high resistivity.

Figure 4a portrays the resistivity model (west-east traverse 1) along the dumpsite with three distinct geo-electric layers: topsoil, lateritic/weathered rock, and fresh basement rock. This traverse is the closest to the dumpsite, extending approximately 150 m in the W – E direction. The profile intersects the dumpsite around 4 – 50 m. The resistivity values span from 2.08 to 221  $\Omega$  m. The upper segment of the profile (horizontal distance 1m to 110m) encompasses resistivity values ranging between 15.4 – 114  $\Omega$ m. These values are attributed to the presence of non-degradable waste materials mixed with clayey sand and clayey laterite, occurring to a depth of about 1.30 m. Beneath this layer lies a conductive zone exhibiting low resistivity values (2.08 – 7.9  $\Omega$ m) within lateral distances of 3 to 61 m, and at depths of 1.5 m – 4.8 m (dumpsite area). Within the range of horizontal distance 62 to 113 m, resistivity values between 15.4 and 58.3  $\Omega$ m are likely due to the presence of clayey material. Notably, near the horizontal distance of about 100 m – 115 m, low resistivity values (2.08 – 4.06  $\Omega$ m) indicate a typical shallow aquifer. Towards the profile's end, at approximately 113 m horizontal distance and a vertical depth of 2.0 m to deeper levels, the resistivity values predominantly exceed 200  $\Omega$ m, suggesting the presence of clay or a typical weathered hard rock. Figure 4b showcases the model resistivity section for Traverse 2, located about 20 m south of and parallel to Traverse 1. The resistivity distribution throughout the profile ranges from 4.4 to 69.8  $\Omega$ m. The resistivity variation reveals inhomogeneity within the upper layer, which is approximately 3 m thick. However, the attributed presence of non-degradable waste materials on Traverse 1 is discontinuous on this Traverse. Within the range of horizontal distances 45 to 114 m, and at relative depths of 0.25 to 0.8 m (topsoil), a low resistivity anomaly is observed, with resistivity values between 4.40 and 9.69  $\Omega$ m. This anomaly is attributed to a small dumpsite and a septic tank along this section. Additionally, resistivity values ranging from 14.4 to 31.7  $\Omega$ m in this layer are indicative of clayey sand, which is underlain by a more resistive layer, with resistivity values reaching about 70  $\Omega$ m. It signifies clay lenses potentially acting as a barrier against leachate migration. This trend generally suggests an increase in resistivity with depth across the profile. Traverse 4 Figure 4c is also parallel to and located about 15 m north of Traverse 1. It is within the abattoir and hosts a mini dumpsite to the extreme. Its top hard pan is characterized as a low-lying coarse-grained banded rock outcrop with a resistivity range between 49.6 and 108  $\Omega$ m. At about 2 m deep, the resistivity values dropped to 7.02 and 15.3  $\Omega$ m, which is attributable to the near-surface water table or runoff within a slope. However, it is also underlain by weathered/fresh basement rock with resistivity range above 200  $\Omega$ m. Traverse 3 Figure 4d is in a N – S azimuth, the only perpendicular profile to others and at about 70 m away from the dumpsite.

Table 2. Physicochemical parameters of well water, leachate and soil samples.

Parameters	Well water	Leachate	Soil	Standard values for drinking water
Appearance	Colourless	Blackish	Blackish	-
Odor	Odourless	Sewage smell	Sewage smell	-
pH	7.66	7.78	7.50	*(6.5-8.5)
Turbidity (NTU)	0.88	5.17	-	
Electrical conductivity (µs/cm)	25.70	46.90	218.00	1000*(2500)
Chloride ion (mg/L)	7.20	8.08	6.60	250*
Sulphate (mg/L)	21.40	42.18	68.22	200 *(250)
Nitrate (mg/L)	0.98	2.90	5.10	45*(50)
Phosphate (mg/L)	0.001	0.06	1.18	(5)
Total acidity	0.44	1.00	0.24	-
Magnesium (mg/L)	0.80	1.00	1.42	(150)
Calcium (mg/L)	6.00	7.40	1.828	(200)
Available phosphorus (%)	0.001	0.04	52.90	(1)
Total Nitrogen (%)	0.001	0.03	0.225	(10)
Total Dissolved Solid (mg/L)	12.70	234.00	180.00	2000*(500)
Total Suspended Solid (mg/L)	2.84	36.78	-	(50)
Total Solid (mg/L)	15.54	270.78	-	(300)
Carbonate (mg/L)	0.432	0.888	0.360	(200)
Bicarbonate (mg/L)	0.8784	1.8056	0.732	(150)
Organic matter (%)	0.3458	0.795	3.890	(2)
Total Organic Carbon (TOC) (%)	0.20	0.46	2.25	(2)
Sodium ion (mg/L)	0.02	0.08	1.432	(200)
Potassium (mg/L)	0.01	0.06	2.084	(12)
Total Alkalinity (mg/L)	0.72	1.48	0.60	(200)
Cation Exchangeable capacity (mg/g)	-	-	7.004	-

( ) = World Health Organization, 2009 (WHO) and \* = United States Environment Protection Agency

Table 3. Contamination factor and Pollution Load Index of heavy metals in soils of Ipata market

Sample	Contamination Factor										PLI
	As	Cd	Cr	Co	Cu	Fe	Mn	Ni	Pb	Zn	
Sample A	3.98	15.38	0.24	0.59	0.13	0.003	0.025	0.23	0.25	0.28	0.18
Sample B	1.42	17.44	0.85	0.68	1.19	0.014	0.061	0.33	0.51	0.52	0.43

Table 4. Ecological risk factor and potential ecological risk index of heavy metals in soil from Ipata market.

Sample	Ecological Risk Factor										RI	Ecological Risk
	As	Cd	Cr	Co	Cu	Fe	Mn	Ni	Pb	Zn		
Sample A	39.8	461.4	0.48	1.18	0.65	0.003	0.025	1.15	1.25	0.28	506.22	High
Sample B	14.2	523.2	1.70	1.36	5.95	0.014	0.061	1.65	2.55	0.52	551.21	High

The top moisturized soil has low resistivity range within 2.08 – 7.9 Ωm and is underlain by weathered/fresh basement rock.

This is a statement that a study shPotential Ecological Risk Index (RI) estimates the overall harmful effects of different

heavy metals in soil [31] using equation (7). RI are classified as: Low risk (RI<150), moderate risk (150≤RI<300), high risk (300≤RI<600) and very high risk (RI≥600) [31, 41].ould not be considered scientific literature. This might be due to a va-

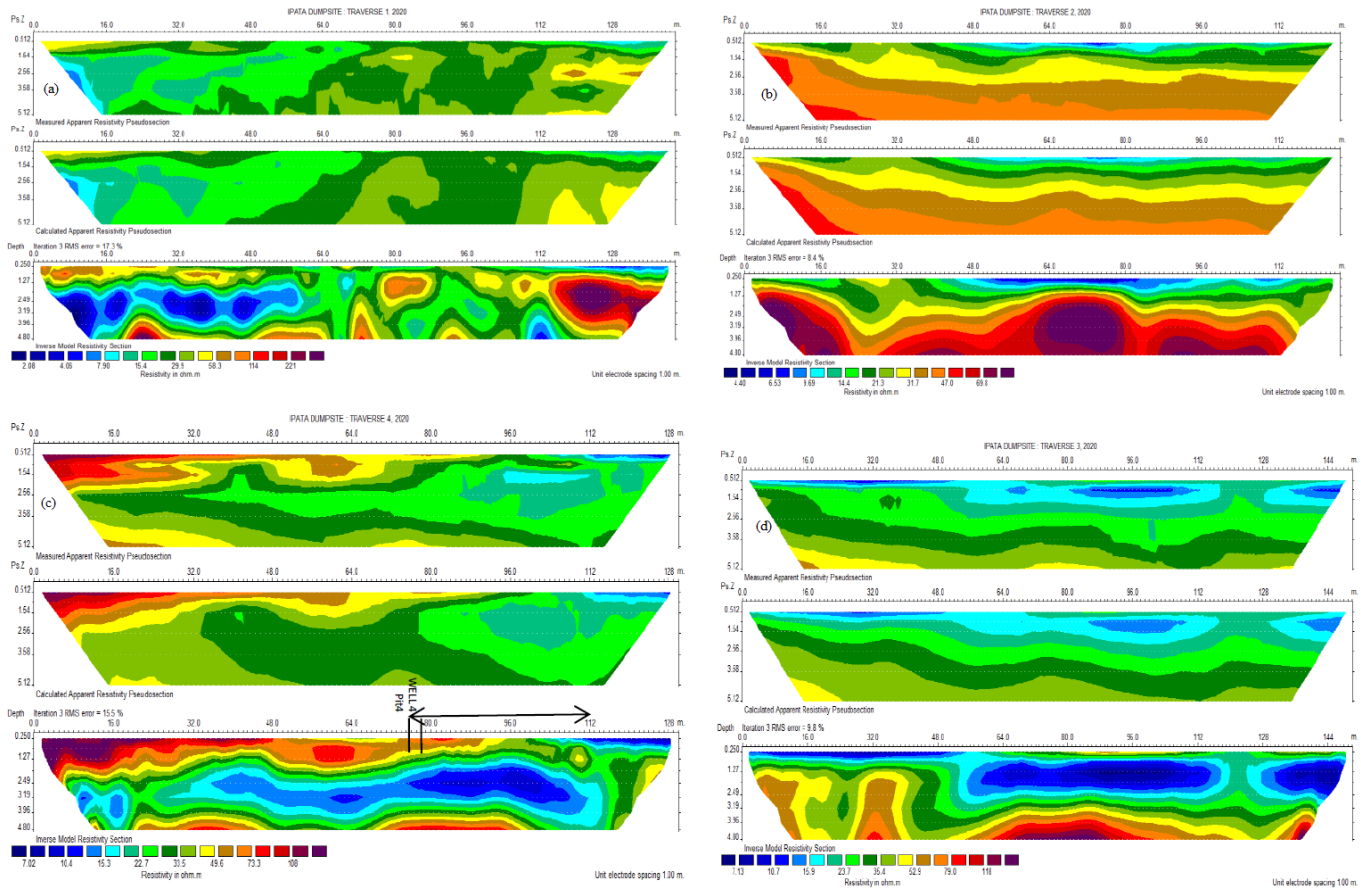


Figure 4. (a) Resistivity model of traverse 1 along the dumpsite, showing the location of pit 1, a shallow hand-dug well and its water level, (b) Resistivity model of traverse 1 along the dumpsite, showing the location of pit 1, a shallow hand-dug well and its water level, (c) Resistivity model of Traverse 4 along the abattoir and dumpsite, showing the location of pit 4, a shallow hand-dug well and its water level at about 2.3 m, (d) Resistivity model of Traverse 3 along the low land/slope, showing the imprint of water percolation beneath the sandfill topsoil.

riety of factors, including the presentation of erroneous results and the inclusion of previously published results in a substantially similar format. The details of article retracted shall not be deleted from the online journal web-portal to preserve the honesty of the record, but it is given notice of retraction. When writers find significant scientific flaws, retractions are occasionally issued by the authors; in other circumstances, the editors determine that retraction is necessary. In every situation, the retraction explains why such action was taken and who is to blame.

### 3.1. Soil Permeability

The soil samples from pits 1 to 4 were analyzed for their grain size composition. Gravel content was found to be 0% in all samples. Sand content ranged from 7% (lowest in pit 3) to 58% (highest in pit 4). Silt content varied from 28% (lowest in pit 3) to 45% (highest in pit 4), while clay content ranged from 12% (lowest in pit 4) to 65% (highest in pit 3) Figure 5. These variations indicate uneven soil distribution and suggest poor grading near the surface. The soil samples are classified using USCS soil classification as impervious to very-impervious CL, ML, and CH, with fines (clay and silt) ranging from 12%

to 65%, highest at greater depths Figure 6. The fines content exceeds the recommended  $\geq 50\%$  for clay liner materials, indicating unsuitability for preventing leachate percolation near the surface but effectiveness at deeper depths. Liquid limits ranged from 18.92% (pit 1) to 54% (pit 3), generally suitable for low hydraulic conductivity and leachate prevention. However, pit 1 fell slightly below the 20% recommended for liner materials, indicating limitations near the surface. The recommended maximum coefficient of permeability value is  $1.0 \times 10^{-7}$  cm/s for landfill barrier soil sets a crucial standard for assessing the suitability of soils to prevent leachate migration in a landfill setting. From the permeability data obtained in pits 2, 3, and 4, it is evident that these locations exhibit varying degrees of permeability, which has significant implications for their effectiveness as barrier materials in landfill construction. In pit 2, the permeability values range between  $3.34 \times 10^{-5}$  cm/s,  $3.23 \times 10^{-5}$  cm/s, and  $3.13 \times 10^{-5}$  cm/s for samples 1, 2, and 3, respectively. These values, while higher than the recommended threshold, are still within the category of low permeability. This suggests that the soils in pit 2 possess some capacity to impede leachate migration but may not provide an ideal barrier against it. Therefore, the suitability of these soils as barrier materials is

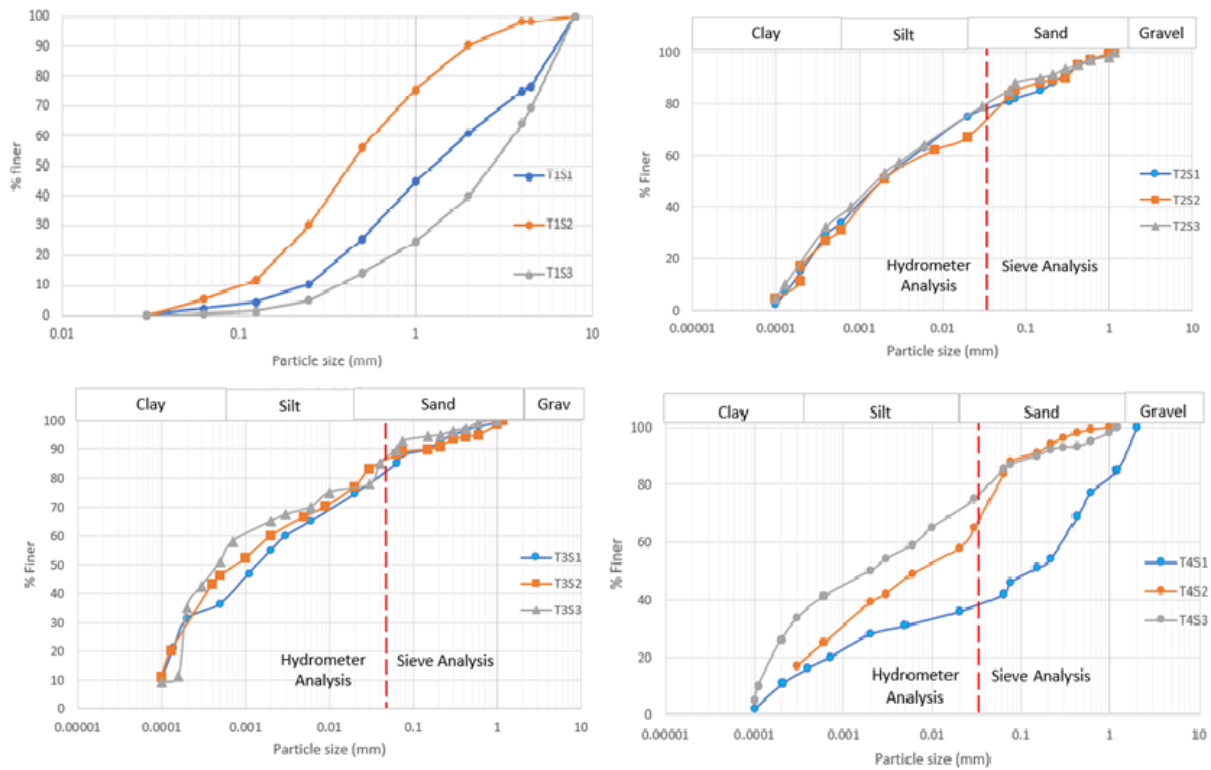


Figure 5. Grain size analysis stack for samples 1, 2 and 3 from (a) pit 1; (b) pit 2; (c) pit 3; and (d) pit 4.

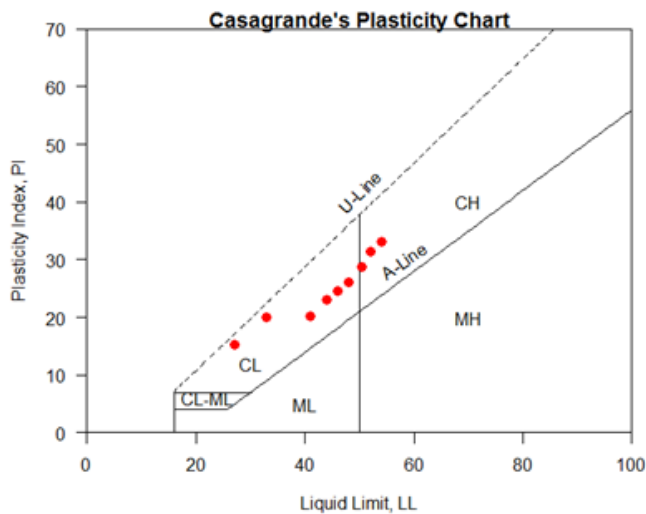


Figure 6. Plasticity Chart for the soil samples: CL-inorganic clays of low plasticity (impervious); ML-inorganic silt of low plasticity (impervious); and CH-inorganic clays of high plasticity.

somewhat limited. In pit 3, the situation is more favorable for landfill applications. The permeability values in this pit range from  $2.98 \times 10^{-6}$  cm/s,  $2.75 \times 10^{-6}$  cm/s, to  $2.52 \times 10^{-6}$  cm/s for samples 1, 2, and 3, respectively. These values fall within the category of very low permeability, indicating that the soils in pit 3 have a significantly higher potential to serve as a moderate

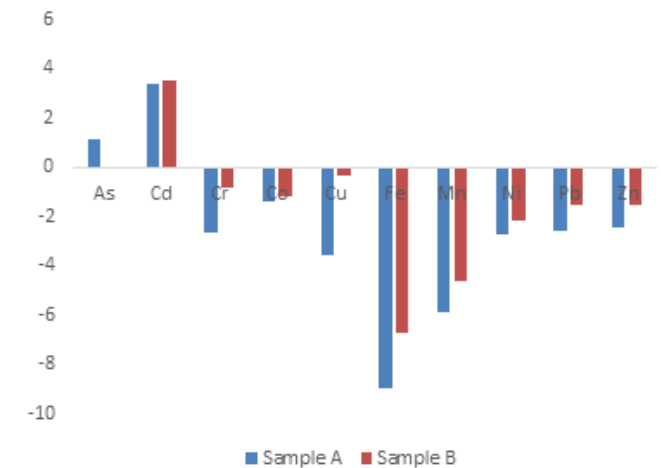


Figure 7. Geochemical analysis results, showing  $I_{geo}$  in both samples.

barrier against leachate migration. Consequently, this pit offers a more promising option for landfill liner materials, especially in areas where stringent leachate containment is necessary.

In contrast, pit 4 presents a mixed picture. The permeability values range between  $3.56 \times 10^{-2}$  cm/s,  $3.72 \times 10^{-4}$  cm/s, and  $3.52 \times 10^{-5}$  cm/s for samples 1, 2, and 3, respectively. While some values are extremely high and not suitable for barrier materials, other values are in the medium to low permeability

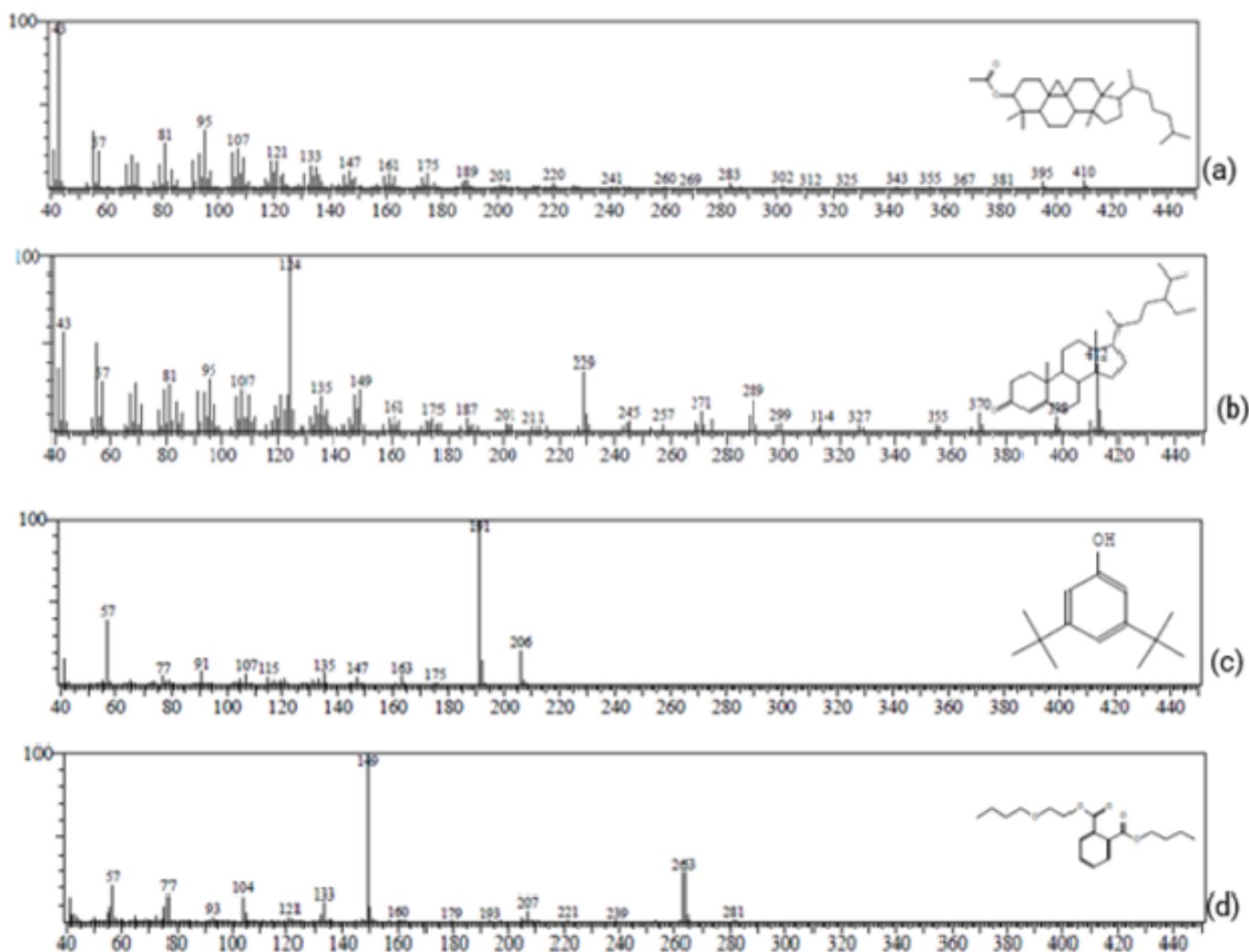


Figure 8. Chromatogram of (a) 9,19-Cyclolanostan-3-ol, acetate, (3.β.)- (b) stigmast-4-en-3-one, (c) 1,2-Benzenedicarboxylic acid and (d) 2-butoxyethyl butyl ester, from the topsoil and leachate.

range. This suggests that pit 4 may have layers of soil with varying permeability characteristics, making it less consistent as a barrier material. Careful selection and assessment of specific layers within pit 4 may be necessary to determine their suitability for landfill applications. The permeability analysis indicates that pit 3 offers the most promising soil characteristics for use as landfill barrier material due to its very low permeability values. Pit 2, while falling within the low permeability range, may be considered as an option with certain limitations. Pit 4's suitability is more complex, requiring a detailed examination of specific layers to identify potential barrier materials. Overall, the choice of soil for landfill liner construction should be guided by the specific requirements of the site and the need for effective leachate containment. Shrinkage values were generally low, suggesting minimal swelling potential. However, the plasticity index and shrinkage limit relationship indicate some areas with a high swelling potential, unsuitable for landfill liners. Permeability values varied across pits, with pit 3 exhibiting

very low permeability, making it a better liner for leachate prevention compared to pits 2 and 4. Water levels in these shallow wells are accessible without deep digging. However, the shallow well water levels are within the poorly graded and pervious topsoil, indicating a limited ability to impede leachate migration.

### 3.2. Physicochemical parameters

The pH value is a crucial indicator of water quality, revealing the presence of acidity or alkalinity. It also influences chemical reactions, including metal toxicity and solubility [34]. The pH levels in Table 2 range from 7.50 to 7.78, well within the acceptable pH range of 6.5 – 8.5 as recommended by WHO (2008) and USEPA (2009) for drinking water. Leachate exhibits the highest pH value, suggesting elevated levels of bicarbonates (1.8056 mg/l) and carbonates (0.888 mg/l) at the site. This is positively correlated with the electrical conductivity (EC) values, with the soil sample having the highest EC

(218  $\mu\text{s}/\text{cm}$ ) due to a greater number of ions. Notably, all EC values for the three samples fall below the USEPA maximum limit of 2500  $\mu\text{s}/\text{cm}$ . The high pH in leachate indicates a significant presence of total dissolved solids (TDS), aligning with the observed TDS value for leachate (280 mg/l). Furthermore, total suspended solids are more pronounced in leachate (36.78 mg/L) compared to well water (2.84 mg/L), indicating higher turbidity in the leachate. Total organic carbon (TOC) remains within the permissible limit (2%) for drinking water. Anions analysis reveals that sulphate ions are the most concentrated in the samples, while chloride, nitrate, and phosphate ions remain relatively low across all samples. Elevated sulphate levels may originate from domestic waste rich in sulphate ions. Sulphate values for well water, leachate, and soil at the site are 21.40 mg/L, 42.18 mg/L, and 68.22 mg/L, respectively, all well below the WHO/USEPA maximum limit of 250 mg/L for safe drinking water.

### 3.3. Heavy Metals

In Figure 7, Cadmium (Cd) exhibited the highest  $I_{geo}$  values in both samples (3.36 and 3.56), while Iron (Fe) had the lowest (-8.97 and -6.70). The elevated  $I_{geo}$  values for Cd in the soil sample from Ipata market indicate significant soil pollution with Cd, primarily due to anthropogenic activities. These findings align with previous studies by Ohiagu *et al.* and Sulaiman *et al.* [35, 42, 43]. Cd also displayed the highest Contamination Factor (CF) values for both samples, while Fe had the lowest CF values. Besides Cd and As, all other metals studied showed minimal contamination at the site. Pollution Load Index (PLI) values of 0.18 and 0.43, both below 1, classify the site as uncontaminated Table 3. These results concur with Alahabadi & Malvandi [36]. The potential ecological risk posed by the studied metals was assessed using Enrichment (E) and Risk Index (RI). All measured metals, except Cd, showed low ecological risk in both samples. Cd, on the other hand, posed a very high ecological risk, resulting in a high potential ecological risk index for both samples Table 4. This aligns with findings from [36, 44]. Two polyaromatic hydrocarbon compounds (from topsoil and leachate) were identified, accounting for 100% of the composition. They were identified as Stigmast-4-en-3-one (74.99%) and 9,19-Cyclolanostan-3-ol, acetate, (3.β.)- (25.01%) and Phenol, 3,5-bis(1,1-dimethylethyl)- (87.07%) and 1,2-Benzenedicarboxylic acid, 2-butoxyethyl butyl ester (12.93%) Figures 8 a-b.

## 4. Conclusion

In an attempt to address the significant threat of leachate from dumpsites to shallow aquifers and its potential impact on human health and the environment. This study employs geophysical methods, particularly 2D Electrical Resistivity Tomography (ERT), soil classification, and various physicochemical tests to assess soil and water quality. The ERT data provided information regarding the subsurface layers and possible groundwater contamination beneath the decomposed topsoil to about 1.2 m by hosting pervious rock/soil with a low resistivity value that ranges from 6.53 to 10.7  $\Omega\text{m}$  underlain by a thin

layer of about 0.5 m thick sandy-clay, suggesting a potential risk of leachate percolation into groundwater. Soil classification indicated a 1.0 m topsoil depth with insufficient clay content to impede leachate percolation because the percentage of the obtained fines falls below the recommended values of the specified liner clay materials. However, the limit of shrinkage within the area shows that the samples have a low potential for swelling, with values falling below <15%. The particle size distribution results show a correlation between the plasticity index classifications. The shrinkage limit and permeability result show that the soil has low-swelling potential with low permeability values ranging from 2.510 to  $3.7 \times 10^{-4}$  cm/sec, and it is within the range of 10.5 to 10.7 that classify the soil as low permeable, suggesting a reduced risk of leachate penetration to greater depths.

The assessment of physicochemical parameters in leachate, well water, and soil has revealed variations in key indicators such as pH, electrical conductivity, total dissolved solids, and anion concentrations. Leachate, characterized by its high pH and electrical conductivity, signifies the presence of elevated total dissolved solids. The well water, although influenced by leachate, generally falls within acceptable pH limits for drinking water. However, the presence of sulfate ions indicates potential contamination from domestic waste sources. Heavy metal concentrations were found to exceed WHO permissible limits in the topsoil, leachate, and well water. Pollution Load Indices classified the site as uncontaminated, except for cadmium, which exhibited a high potential ecological risk. This highlights the complex interplay between heavy metal contamination and ecological impact. Also, the absence of listed persistent organic pollutants (POPs) in the analyzed samples suggests that, while heavy metals are a concern, the site does not currently exhibit a significant presence of POPs. This implies that the findings of this study underscore the urgent need for proactive pollution abatement measures in urban dumpsites like Ipata. Regular monitoring of surface water and groundwater quality in and around dumpsites is imperative to safeguard public health and environmental integrity. Additionally, the multidisciplinary methodologies employed in this research serve as a valuable guide for future assessments of leachate contamination in urban environments, contributing to effective waste management practices and sustainable urban development.

## Acknowledgment

The authors appreciate the financial support of the Nigerian Tertiary Education Trust Fund 2020 Institutional Based Research grant (KWA-SUIBR/CSP/090320/VOL7/TETF2019/0096) and Kwara State University Centre for Research and Development

## References

- [1] S. Mor, & K. Ravindra, "Leachate characterization and assessment of groundwater pollution near municipal solid waste landfill site", *Environ. Monitor & Assess* **118** (2006) 435. <https://doi.org/10.1007/s10661-006-1505-7>.

- [2] V. Naudet, J. Gourry, J. Girard, F. Mathieu, & A. Saada, "3D electrical resistivity tomography to locate DNAPL contamination around a housing estate," *Near surface Geophysics* **bf12** (2013) 351. <https://doi.org/10.3997/1873-0604.2012059>.
- [3] K. D. Oyeyemi, A. P. Aizebeokhia, A.N. Ede, O.J. Rotimi, O. A. Sanuade, O.M. Olofinnade, O.A. Akhaguere, & O. Attat, "Investigating the near surface leachate movement open dumpsite using surficial ERT method," *IOP Conf. Ser. Mater. Sci. Eng.* **640** (2019) 012109. <https://doi.org/10.1088/1757-899x/640/1/012109>.
- [4] F. Parvin, & S. M. Tareq, "Impact of landfill leachate contamination on surface and groundwater of Bangladesh: a systematic review and possible public health risks assessment," *Appl Water Sci* **11** (2021) 100. <https://doi.org/10.1007/s13201-021-01431-3>.
- [5] G. Badmus, O. Ogungbemi, O. Enuiyin, J. Adeyeye, & A. Ogunyemi, "Delineation of leachate plume migration and appraisal of heavy metals in groundwater around Emirin dumpsite, Ado-Ekiti, Nigeria," *Scientific African* **17** (2022) e01308. <https://doi.org/10.1016/j.sciaf.2022.e01308>
- [6] J. Zume, A. Tarhule, & S. Christenson, "Subsurface imaging of an abandoned solid waste landfill site in Norman, Oklahoma," *Groundwater Monitoring and Remediation* **26** (2006) 62. <https://doi.org/10.1111/j.1745-6592.2006.00066.x>
- [7] O. Osinowo, & A. Olayinka, "Very low frequency electromagnetic (VLF-EM) and electrical resistivity (ER) investigation for groundwater potential evaluation in a complex geological terrain around Ijebu-ode transition zone, Southwestern Nigeria," *J. Geophys. & Eng.* **9** (2012) 374. <https://doi.org/10.1088/1742-2132/9/4/374>.
- [8] N. K. Olasunkanmi, Z. M. Usman, & A. A. Jimoh, "Investigation of groundwater quality around municipal waste disposal site in Malete southwestern Nigeria," *Arabian Journal of Geosciences* **16** (2023) 273. <https://doi.org/10.1007/s12517-023-11359-4>.
- [9] A. Macdonald, H. Bonsor, E. Dochartah, & R. Tailor, "Quantitative map of groundwater resources in Africa," *Environ. Res. Lett.* **7** (2012) 024009. <https://doi.org/10.1088/1748-9326/7/2/024009>.
- [10] C. Bernstone & T. Dahlin, "DC resistivity mapping of old landfills: two case studies," *Eur. J. Environ. Eng. Geophys.* **2** (1997) 121. [https://www.researchgate.net/publication/290694802\\_DC\\_resistivity\\_mapping\\_of\\_old\\_landfills\\_Two\\_case\\_studies](https://www.researchgate.net/publication/290694802_DC_resistivity_mapping_of_old_landfills_Two_case_studies)
- [11] C. Bernstone, T. Dahlin, T. Ohisso, & W. Hogland, "DC resistivity mapping of internal Landfill structure: two pre-excavation surveys," *Environmental Geology* **39** (2000) 360. <https://doi.org/10.1007/s002540050015>.
- [12] A. Sina, N. Reyhaneh, Z. Amin, F. Hassan, & G. Reza, "Experimental investigation of correlations between electrical resistivity, moisture content and voltage values for leachate contaminated clayey sand," *Journal of Applied Geophysics* **193** (2021) 104391. <https://doi.org/10.1016/j.jappgeo.2021.104391>.
- [13] M. A. Adabanija, "Spatio-temporal monitoring of leachates dispersion beneath a solid wastes dump in a basement complex of southwestern Nigeria," *Journal of Applied Geophysics* **210** (2023) 104953. <https://doi.org/10.1016/j.jappgeo.2023.104953>.
- [14] A. Binley, G. Cassiani, R. Middleton, & P. Winship, "Vadose zone flow model parameterisation using cross-borehole radar and resistivity imaging," *Journal of Hydrology* **267** (2002) 147. [https://doi.org/10.1016/S0022-1694\(02\)00146-4](https://doi.org/10.1016/S0022-1694(02)00146-4).
- [15] S. K. Sandberg, L. D. Slater, & R. Versteeg, "An integrated geophysical investigation of the hydrogeology of an anisotropic unconfined aquifer," *Journal of Hydrology* **267** (2002) 227. [https://doi.org/10.1016/S0022-1694\(02\)00146-4](https://doi.org/10.1016/S0022-1694(02)00146-4).
- [16] I. Abdulganiyu, A. A. Olukole, L. U. John, C.A. Nelson, & O. O. Raheem, "Detection of groundwater level and heavy metal contamination: A case study of Olubunku dumpsite and environs, Ede North, Southwestern Nigeria," *Journal of African Earth Sciences* **197** (2022) 104740. <https://doi.org/10.1016/j.jafrearsci.2022.104740>.
- [17] W. Daily, A. Ramirez, & R. Johnson, "Electrical impedance tomography of a perchloroethylene release," *Journal of Environmental and Engineering Geophysics* **2** (1998) 189. <https://doi.org/10.2172/461374>.
- [18] B. J. M. Goes, & J. A. C. Meekes, "An effective electrode configuration for the detection of DNAPLs with electrical resistivity tomography," *Journal of Environmental and Engineering Geophysics* **9** (2004) 127. <https://doi.org/10.4133/JEEG9.3.127>.
- [19] K. Reddy, H., Hettiarachchi, N. Parakalla, & J. Gangathulasi, J. "Geotechnical Properties of Fresh Municipal Solid waste at Orchard Hills Landfill, USA," *Waste Management* **29** (2008) 952. <https://doi.org/10.1016/j.wasman.2008.05.011>.
- [20] L. De Carlo, M. Perri, M. Caputo, R. Deiana, M. Vurro, & G. Casiani, "Characterization of a dismissed landfill via electrical resistivity tomography and mise-a-lamasse method," *J. Appl Geophys* **98** (2013) 1. <https://doi.org/10.1016/j.jappgeo.2013.07.010>.
- [21] C. Moreira, A. Braga, L. Godoy, & D. Sardinha. "Relationship between age of waste and natural electric potential generation in sanitary landfill," *Geofisica Int.* **52** (2013) 375.
- [22] E. A. Ayolabi, L. B. Oluwatosin, & C. D. Ifekwuna, "Integrated geophysical and physiochemical assessment of Olushosun sanitary landfill site, southwest Nigeria," *Arab J. Geoscience*, **8** (2015) 4101. <https://doi.org/10.1007/s12517-014-1486-8>.
- [23] S. Park, Y. Myeong-jong, & K. K. Jung-HoSeung-Wook, "Electrical resistivity imaging (ERI) monitoring for groundwater contamination in an uncontrolled landfill, South Korea," *Geophysics J Applied Geophysics* **135** (2016) 1. <https://doi.org/10.1016/j.jappgeo.2016.07.004>.
- [24] A. Arato, M. Wehrer, & B. Biró, *et al.* "Integration of geophysical, geochemical and microbiological data for a comprehensive small-scale characterization of an aged LNAPL-contaminated site," *Environ. Sci. Pollut. Res.* **21** (2014) 8948. <https://doi.org/10.1007/s11356-013-2171-2>.
- [25] O. Igwe, E. J. Adepehin, & J. O. Adepehin, "Integrated geochemical and microbiological approach to water quality assessment: case study of the Enyigba metallogenic province, South-eastern Nigeria," *Environ Earth Sci* **74** (2015) 3251. <https://doi.org/10.1007/s12665-015-4363-1>.
- [26] S. A. Ganiyu, B. S. Badmus, & M. A. Oladunjoye, *et al.* "Assessment of groundwater contamination around active dumpsite in Ibadan southwestern Nigeria using integrated electrical resistivity and hydrochemical methods," *Environ Earth Sci* **75** (2016), 643. <https://doi.org/10.1007/s12665-016-5463-2>.
- [27] S. U. Eze, D. O. Ogagarue, & S. L. Nnorom, *et al.* "Integrated geophysical and geochemical methods for environmental assessment of subsurface hydrocarbon contamination," *Environ Monit Assess* **193** (2021) 451. <https://doi.org/10.1007/s10661-021-09219-3>.
- [28] O. O. Okoyomon, H. A. Kadir, Z. U. Zango, U. Saidu, & S. A. Nura, "Physicochemical composition and heavy metal determination of selected industrial effluents of Ibadan city, Nigeria," *Open Journals of Environmental Research (OJER)* **2** (2021) 58. <https://doi.org/10.52417/ojer.v2i2.270>.
- [29] N. G. Obaje, "Geology and mineral resources of Nigeria," *Lecture Notes in Earth Sciences*, Springer Berlin, Heidelberg 2009, pp. 115-115. <https://doi.org/10.1007/978-3-540-92685-6>.
- [30] M. Loke, & R. Barker, "Rapid least-squares inversion of apparent resistivity pseudosections by a quasi-Newton method. *Geophysics Prospect*," **44** (1996) 131. <https://doi.org/10.1111/j.1365-2478.1996.tb00142.x>.
- [31] L. Hakanson, "An ecological risk index for aquatic pollution control. A sedimentological approach," *Water Research* **14** (1980) 975. [https://doi.org/10.1016/0043-1354\(80\)90143-8](https://doi.org/10.1016/0043-1354(80)90143-8).
- [32] D.P.R. "Department of petroleum resources, Lagos, Nigeria" 1980. <https://dpr.gov.ng/index.php.1980>.
- [33] K. K. Turekian, & K. H. Wedepohl. "Distribution of the elements in some major units of the Earth's crust," *Bulletin of Geological Society of America* **72** (1961) 175. [https://doi.org/10.1130/0016-7606\(1961\)72\[175:DOTEIS\]2.0.CO;2](https://doi.org/10.1130/0016-7606(1961)72[175:DOTEIS]2.0.CO;2)
- [34] S. S. Dada, I. A. Tubosun, J. R. Lancelot, A. U. Lar, "Late Archaean U-Pb age for the Reactivated Basement of Northeastern Nigeria," *Journal of African Earth Science* **16** (1993) 405. [https://doi.org/10.1016/0899-5362\(93\)90099-C](https://doi.org/10.1016/0899-5362(93)90099-C).
- [35] Ohiagu F.O., Lele K.C., Chikezie P.C. *et al.* "Pollution Profile and Ecological Risk Assessment of Heavy Metals from Dumpsites in Onne, Rivers State," *Nigeria Chemistry Africa* **4** (2021) 207. <https://doi.org/10.1007/s42250-020-00198-5>.
- [36] A. Alahabadi, & H. Malvandi, "Contamination and ecological risk assessment of heavy metals and metalloids in surface sediments of the Tajan River, Iran," *Marine Pollution Bulletin* **133** (2018) 741. <https://doi.org/10.1016/j.marpolbul.2018.06.030>.
- [37] D. L. Tomlinson, J. G. Wilson, C. R. Harris, *et al.* "Problems in the assessment of heavy-metal levels in estuaries and the formation of a pollution index," *Helgolander Meeresunters* **33** (1980) 566. <https://doi.org/10.1007/BF02414780>.
- [38] G. Muller, "Index of geoaccumulation in sediments of the Rhine River,"

- Geo Journal **2** (1969) 108. <https://www.scienceopen.com/document?vid=4b875795-5729-4c05-9813951e2ca488>.
- [39] G. Muller, "Heavy metals in the sediment of the Rhine-changes seity," *Umschau in Wissenschaft Und Technik* **79** (1979) 778–783. <https://www.scirp.org/reference/ReferencesPapers?ReferenceID=1340468>.
- [40] E. Orellana-Mendoza, R. R. Acevedo, C. H. Huamán, Y. M. Zamora, M. C. Bastos, & H. Loardo-Tovar, "Ecological Risk Assessment for Heavy Metals in Agricultural Soils Surrounding Dumps, Huancayo Province, Peru," *Journal of Ecological Engineering* **23** (2022) 75. <https://doi.org/10.12911/22998993/147809>.
- [41] J. Hilton, W. Davison, & U. Ochsenein. "A mathematical model for analysis of sediment coke data," *Chem Geol* **48** (1985) 281. [https://doi.org/10.1016/0009-2541\(85\)90053-1](https://doi.org/10.1016/0009-2541(85)90053-1).
- [42] A. Enuneku, E. Biose, & L. Ezemonye, "Levels, distribution, characterization and ecological risk assessment of heavy metals in road side soils and earthworms from urban high traffic areas in Benin metropolis, Southern Nigeria," *Journal of Environmental Chemical Engineering* **5** (2017) 2773. <https://doi.org/10.1016/j.jece.2017.05.019>.
- [43] M. B. Sulaiman, K. Salawu, & A. U. Barambu, "Assessment of concentrations and ecological risk of heavy metals at resident and remediated soils of uncontrolled mining site at Dareta Village, Zamfara, Nigeria," *J Appl Sci Environ Manag* **23** (2019) 187. <https://doi.org/10.4314/jasem.v23i1.28>.
- [44] B. Mugosa, D. Durovic, N. Vukovic, M. S. Barjaktarovic'-Labovic, & M. Vrvic, "Assessment of ecological risk of heavy metal contamination in coastal municipalities of Montenegro," *Int J Environ Res Public Health* **13** (2016) 393. <https://doi.org/10.3390/ijerph13040393>.